Numerical and Experimental Studies of Rotorcraft Icing Phenomena

Jeewoong Kim and Lakshmi Sankar
School of Aerospace Engineering, Georgia Institute of Technology, Atlanta, GA 30332, USA

Jose Palacios
Department of Aerospace Engineering, The Pennsylvania State University, PA 16803, USA

Richard E. Kreeger
NASA Glenn Research Center, Cleveland, OH, 44135, USA

Abstract

With support from and collaboration with NASA and the DoD's Vertical Lift Research Center of Excellence, research teams at Georgia Institute of Technology and The Pennsylvania State University are conducting computational and experimental studies on ice accretion for representative 2-D and 3-D configurations. A wealth of data including ice shapes, surface pressure data, and 3-D performance data (such as sectional lift, drag, thrust, torque) are being acquired. Details of the ice modelling tools are presented along with selected validation studies. Advantages and shortcomings of the methods are discussed as are our teams' prospects for the future.

1. Introduction

Operation of rotorcraft under icing conditions is a challenging problem that affects the availability, affordability, safety and survivability of the vehicle. Availability of the vehicle may be compromised if the ice formation requires excessive torque to overcome the drag needed to operate the rotor. Affordability is affected by the power requirements and cost of ownership of the deicing systems needed to safely operate the vehicle. In order to ensure safety, ice shedding should also be addressed. Given the importance of understanding the effects of icing on rotorcraft performance and certification, considerable work has been done over the past two decades on the development of analytical and empirical tools, accompanied by high quality wind tunnel and flight test data.

Modeling the physics of this complex phenomenon requires tools from the disciplines of computational fluid dynamics, computational structural dynamics, ice accretion models and ice shedding models. The individual modules need to be robust, must be compatible with each other permitting industry-standard input-output exchange, and should be modular in order to allow the replacement of the individual modules with more advanced modules as the underlying technology matures. The coupled analysis should be applicable to 2-D airfoils, airframe, and 3-D rotors in hover and forward flight under icing conditions, and be well correlated with test data.

To address this need for advanced computational tools, under the direction of NASA Glenn Research Center, a suite of computer codes for modeling icing on 2-D and 3-D configurations have been developed and are in extensive use in industry. The earliest of these is LEWICE, now in version 3.2.2. Three-dimensional configurations may be handled in a strip theory fashion in a version of LEWICE known as LEWICE3D. Recently, an advanced ice accretion analysis has been developed in which the trajectory analyses use velocity fields from Navier-Stokes solutions (structured or unstructured). Previous methods relied on a potential flow (panel method) based velocity field trajectories. Advanced toolkits have also been developed, which take the output from LEWICE and prepare the airfoil sections for use in CFD analyses.

The present researchers are developing advanced tools for modeling ice accretion [1-9] that build on and complement LEWICE. Validation of these tools requires high quality data for ice shapes and associated airloads. An excellent set of test data is available from NASA Glenn for a variety of configurations [10,11]. Researchers at Penn State University have also obtained high quality ice shape data, and associated airloads data for a series of 2-D (airfoil), and 3-D (rotor in hover and forward flight) configurations [12,13]. This paper gives a detailed description of the complementary ice accretion models being developed. Selected results are presented that demonstrate and validate these methods.

2. Computational Methodologies

Current Computational ice accretion modeling methods address some or all of the sub-disciplines of mesh generation, compressible aerodynamic CFD of the air flow, modeling of the kinematics, dynamics and thermodynamics of the droplets and liquid films, and,

freezing and growth of the ice shape itself. These elements of the overall analysis are complicated by their inherent coupling, which can be accommodated loosely or strongly in the computational procedure. Also, ice accretion is a multi-time scale problem, with an aero-thermodynamic time-scale on the order of 10^{-4}-10^{-3} s, and accretion time-scale on the order of 10^{1}-10^{2} s, and this scale disparity must be accommodated as well.

The Georgia Tech team uses a loosely coupled approach wherein complimentary sets of computational tools work seamlessly with the LEWICE ice modelling analysis developed at the NASA Glenn Research Center. Figure 1a shows the basic elements of this ice accretion simulation model. The Penn State Team uses both a loosely coupled (similar to Figure 1a) and a strongly coupled approach. In the latter, wherein a single solver performs all of the physics / numerics implicitly, and an Immersed Boundary Method (IBM) is used to evolve the ice shape. Figure 1b shows the basic elements of the strongly coupled ice accretion simulation model.
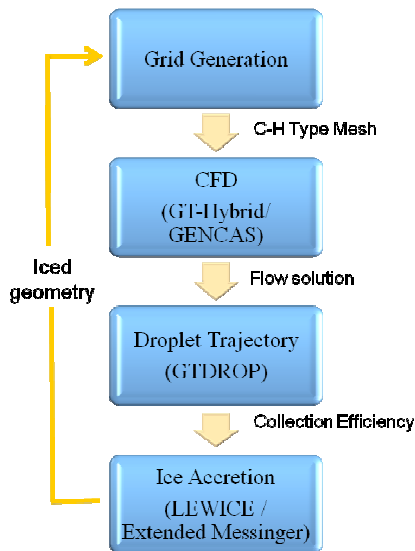

Figure 1a. Overview of the loosely coupled ice accretion analysis.
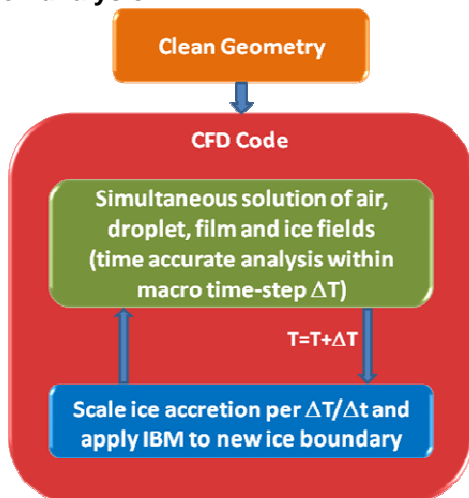

Figure 1b. Overview of the strongly coupled ice accretion analysis.

2-1. CFD solvers

The Georgia Tech team uses a flow solver called GT-Hybrid [14], a finite volume based three-dimensional unsteady viscous compressible flow solver. This analysis performs the costly Navier-Stokes calculations only in the immediate vicinity of the rotor blades. Away from the rotor, the vortex wake is captured using a Lagrangian approach.

This hybrid approach allows for economical modeling of viscous features near the blades, and a "non-diffusive" modeling of the trailing wake in the far field. Figure 2 shows a schematic of the Hybrid method employed in GT-Hybrid, depicting the Navier-Stokes domain around the blade-region, the wake captured inside the near-blade Navier-Stokes domain, and the portion of the wake which is modeled as a Lagrangian free wake.

The influence of the trailed vortices from the wake model on the blade aerodynamics is computed by appropriately specifying the vortex-induced velocities at the far field boundary of the Navier-Stokes domain, neglecting the contribution of the elements captured within the CFD volume grid.
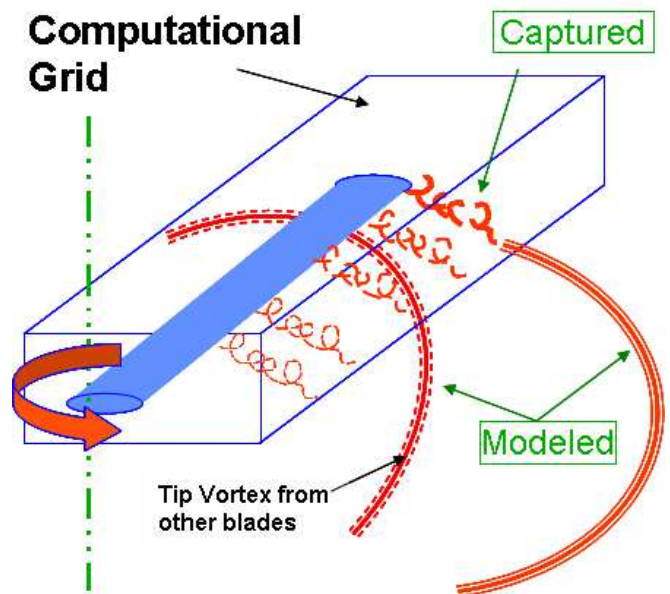

Figure 2. A Schematic View of the Hybrid Method.

2-2. Droplet Solver

Once the flow field is computed, the next step is to compute the volume fraction of the water droplets and the droplet velocity at the same nodes of the discrete domain where the flow variables of air are known. The Georgia Tech team uses an in-house code called GTDROP [2] that is based on Eulerian approach. In this method, the average water droplet properties within a control volume are solved instead of tracking individual particles. This physical approach has several advantages over the Lagrangian approach. These include improved quality of the solution, the ability to model unsteady flows over bodies in relative motion, and the automated treatment of shadow zones around the rotor where there is no impingement. The interaction between the air particles and the droplets

occurs through a drag force exerted by the mean flow on the particles. The presence of the droplet flow field is, however, not felt by the mean flow field solver, and the droplets are treated as a passive scalar field. When the air flow is steady, the CFD analysis may be computed a priori and used in the droplet solver. If the flow is unsteady, the droplet analysis should be done once every time step, after the mean flow properties are computed.

The governing equations for the conservation of mass and momentum of the droplets are written as follows:

$$\frac{\partial \alpha}{\partial t} + \nabla \cdot (\alpha u_i) = 0 \qquad (1)$$

$$\frac{\partial u_i}{\partial t} + u_i \cdot \nabla u_i = \frac{C_D \, \mathrm{Re}_d}{24K}(u_a - u_i) + \left(1 - \frac{\rho_a}{\rho}\right)\frac{1}{Fr^2} g_i \qquad (2)$$

Here, α is the non-dimensionalized volume fraction of water and u_i is the non-dimensional velocity of droplets.

Additionally, u_a is the non-dimensionalized velocity of air; ρ and ρ_a are the density of water and air, respectively; g_i, is the gravity vector; $F_r = U_\infty / \sqrt{Lg}$ is the Froude number; U_∞ is the speed of air at freestream; L, is the characteristic length (typically the airfoil chord length); $K = \rho d^2 U_\infty / 18L\mu$, is an inertia parameter; and, μ is the dynamic viscosity of air.

The drag coefficient is defined as

$$C_D = \frac{24}{\mathrm{Re}_d}\left(1 + 0.15\,\mathrm{Re}_d^{\,0.687}\right) \qquad \mathrm{Re}_d \leq 1000$$
$$C_D = 0.4 \qquad\qquad\qquad \mathrm{Re}_d > 1000 \qquad (3)$$

with,

$$\mathrm{Re}_d = \frac{\rho_a d U_\infty |u_a - u_i|}{\mu}$$

Equations (1) and (2) are recast in finite volume form using divergence theorem. A first order upwind scheme is employed for computing the mass and momentum flux at the faces of the control volume. An implicit time marching algorithm is employed. Mean flow quantities are lagged by one time step compared to particle velocity and volume fraction. The resulting system of banded linear equations is solved using an approximate factorization scheme.

2-3. Ice Accretion Solver

The present studies were conducted using LEWICE [15] which employs the classical Messinger model, and an in-house methodology developed by the Georgia Tech researchers that employs the extended Messinger model.

2-3-1. LEWICE

LEWICE [15], developed by the NASA Glenn Research Center, has been used by literally hundreds of users in the aeronautics community for predicting ice shapes, collections efficiencies, and anti-icing heat requirements. LEWICE consists of four major modules. The first module is flow field calculation using a panel method, developed by Hess and Smith [16]. The second module is a particle trajectory and impingement calculation using a Lagrangian approach by Frost et al [17]. Thermodynamic and ice growth calculation is done in a third module. An integral boundary layer method is used to determine the skin friction and the local convective heat transfer coefficient. Finally, the classical Messinger model [18] is for ice accretion thermodynamic analysis. LEWICE also has capability for de-icing and anti-icing analyses. All the modules have been seamlessly integrated. The analysis is robust and is capable of modeling 2-D and 3-D configurations ranging from simple airfoils to a complete aircraft configuration.

2-3-2. Extended Messinger Model

The extended Messinger Model [19, 20] is based on the standard method of phase change or the Stefan condition [21], similar to the Messinger [18] energy balance in the form of a differential equation. The Stefan problem consists of four equations: heat equations in the ice and water layers, corresponding mass balance equations, and a phase change or Stefan condition at the ice/water interface. Figure 3 shows some of the details of the extended Messinger's model in one-dimension. The difference relative to the original Messinger model is that the extended Messinger model requires knowledge of the temperature gradients within each layer. The heat equations in the ice and water layer may however be analytically and economically solved, because of their simple forms.

An ice accretion code has been developed based on the extended Messinger formulation shown in Figure 3, with additional details given in Ref. 19 and 20. The boundary layer analysis is done by Thwaites' method for the laminar flow region, and Head's method for the turbulent flow region. Instead of using empirical skin friction equation, skin friction coefficient from CFD simulation is used for the boundary layer and the thermodynamic analysis. Transition location is determined by Von Doenhoff criterion, $\mathrm{Re}_k > 600$, where Re_k is the Reynolds number based on the roughness height and the local edge velocity.

3. Results and Discussions

In this section, selected results of numerical and experimental studies for rotorcraft icing phenomena are presented.

3-1. Ice Accretion on Rotor Blade

Extensive rotor blade ice tests have been done in NASA Glenn's Icing Research Tunnel (IRT) in

September 2013 [22-24]. In the present work, ice growth simulations have been performed for one of the numerous test conditions.

The model rotor is a production of Bell Helicopter Model 206B tail rotor blade with heater blankets bonded to the blade surface. The rotor is a two-bladed teetering rotor with a δ_3 of 45°. The rotor radius is 32.6", a chord of 5.3" and has rectangular blade with NACA0012 airfoil.

The selected test condition is called Run 54. Table 1 shows the corresponding flow conditions. The blade motion (flapping angle) is computed from a coupled CFD / Flapping Dynamics analysis of the clean rotor. Flapping angles of blade are recomputed after each CFD simulation. The calculations are redone using the new flapping angles. The simulations are continued until the hub roll and pitching moments are zeroed out. Figure 4 shows a flowchart of the CFD / Flapping Dynamics analysis.

Table 1. Test Conditions for Run54.

Forward Velocity (knot)	60
RPM	2100
LWC (g/m^3)	0.5
Drop (µm)	15
Temperature (K)	263.15
Time (Min)	1
Collective (Deg.)	8

A C-H grid, 131 (chordwise) x 70(spanwise) x 45 (normal), was used for flow field prediction. The predicted flow field solutions from CFD simulation were fed into an Eulerian droplet model and the two ice accretion codes in order to get the ice shape. A multi-step approach is used with a time step of 15 sec. The ice accretion simulations were conducted at four different azimuthal locations (Ψ = 0°, 90°, 180°, 270°). Unsteady flow field data for the clean rotor was used to compute the collection efficiencies at these azimuthal locations.

Figure 5 shows the comparison of predicted ice shape using two ice accretion codes (LEWICE and Extended Messinger model) at the selected radial locations 37% R, 49% R, 61% R, 74% R, and 86% R, and 98% R. Ice shapes predicted from both approach are smooth and rounded. Marginal difference in ice shape is seen at the inboard between LEWICE and Extended Messinger model. Predicted ice shapes from both approaches are close to experimental ice shape at the inboard region. Ice shapes start to differ towards blade tip. The Extended Messinger model predicts thicker ice near the leading edge of airfoil. The predicted maximum ice thickness from the Extended Messinger model is over-predicted compared to experiment.

In the tip region of helicopter blades at high speed, the effect of kinetic heating affect ice accretion process. In order to consider kinetic heating effect, blade surface temperature distributions which are predicted from CFD simulation were fed into Extended Messinger model. Figure 6 shows the effect of kinetic heating effect on ice accretion on rotor blade. Marginal difference in ice shape is seen at the inboard between two cases. By considering kinetic heating effect, improvement on the prediction of ice shape is seen.

Rotor blade ice tests also have been done in the Adverse Environment Rotor Test Stand Facility at the Penn State University (Figure 7). The accreted ice shapes formed on truncated helicopter rotor blades were hand traced at multiple locations along the span of the rotor. At the tip of the blades, ice shapes were photographed and digitized.

Ice growth simulations have been performed for one of the test conditions, called Test4. Table 2 shows the corresponding test conditions. The rotor tested in the Penn State facility is a two-bladed teetering rotor. The rotor has a rectangular planform, and is made of NACA 0015 airfoil sections. The radius is 46", and the chord is 6.8".

A C-H grid, 131 (chordwise) x 70(spanwise) x 45 (normal), was used for flow field prediction. The predicted flow field solutions from CFD simulation were fed into the present Eulerian droplet model and the ice accretion is subsequently computed. Figure 8 shows the comparison of predicted ice shape using the Extended Messinger model at the blade tip. The Extended Messinger model did a reasonably good job of predicting the ice shape at the nose, but the ice was thicker than expected downstream of the nose region.

Table 2. Test Conditions for Test4.

Flight condition	Hover
RPM	900
LWC (g/m^3)	2.5
Drop (µm)	20
Temperature (K)	263.15
Time (Min)	1
Collective (Deg.)	0

3-2. Rotor Blade Ice Shedding Analysis

Simulations have been done for modeling the ice shedding phenomena. A rotor configuration tested by Fortin [25] was considered. The rotor is a 1/18-scale model of a small helicopter. The rotor diameter is 780 mm, and the tip speed is 130 m/s. The forward speed of the rotor was 15 m/sec, leading to a low advance ratio (forward speed to tip speed ratio) of 0.115. The blades are untwisted, and made of NACA 0012 sections (69.75 mm in chord). The liquid water content was 0.842 g/m3, and the median diameter of the water drops was 26.7 µm. The ambient temperature was parametrically varied between -20 deg Celsius and -5 degree C.

An empirical model for self-shedding [23] was used in present ice shedding simulations. The following procedure used to determine the length of the shed ice and the time at which shedding occurs:

a. At any specified instant in time, the contact area, volume, and mass of the ice are computed. This is done using the simultaneous integration of the flow

equations, structural dynamics equations, and the ice accretion equations in time.

b. The shear stress at the blade surface between the ice mass and the blade and the cohesive stresses exerted on a segment of ice by the neighboring ice mass are computed. The surface shear stresses are based on temperature and on the rotor blade surface ,using relationships derived from experimental data.

c. The components of the centrifugal, shear, and cohesive force vectors are summed up, on sections on the rotor blade.

d. The feasibility of shedding is examined. It is assumed that all the ice mass outboard of a given radial location will be shed if the sum of applied forces (centrifugal, edge cohesion, and optionally aerodynamic pressure) on the mass of ice exceeds the adhesion force.

The accretion time at which such shedding occurs as well as the thickness and length of the shed ice shape was extracted from the present simulations. Figures 9 shows comparisons with experiment for the cases of different ambient temperatures. Reasonably good agreement was found for properties, such as the length of the shed ice and the time at which shedding occurs.

3-3. Rotor Blade De-Icing Simulation

De-icing tests also have been done in NASA Glenn's Icing Research Tunnel (IRT) in September 2013 [22-24]. In the present work, the aerothermal analysis also have been performed by LEWICE and an in-house 3D heat conduction solver developed by the Georgia Tech team. LEWICE uses 2-D strip theory, and solves the heat conduction equations on a Cartesian grid. A fully 3-D heat conduction analysis that acknowledges curvature of the heat elements, and the finite spanwise extent of the heating elements has been developed by Georgia Tech researchers.

One of test conditions, Run33, is selected as a baseline case. This condition is dry air case and used for the validation of the current aerothermal prediction module. Table 3 shows the corresponding test conditions. De-icing simulations have been done at 2D cross section, mid-span. Azimuthally averaged local velocity (210 ft/sec) and pitch angle (2.6 Deg.) are used as a flow condition. Convective boundary condition is applied at boundaries on computational geometry. Heat transfer coefficient (HTC) predicted from LEWICE is used as a boundary condition on external airfoil surface. Figure 10 shows cross section of heater zones. Comparison of blade surface temperature at different locations are seen in Fig. 11 and 12. Numerical prediction shows reasonable peak temperature at location B (leading edge of airfoil) and location C (downstream region).

Table 3. Test Conditions for Run33.

Forward Velocity (knot)	60
RPM	1200
Temperature (°F)	45
Time (Min)	5
Collective (Deg.)	5

4. Summary and Recommendations

A coordinated computational effort by a team of researchers from NASA Glenn Research Center, Penn State, and Georgia Tech is underway to understand the fundamental phenomena of ice formation over rotorcraft airfoil sections. A series of progressively challenging simulations have been carried out. These include ability of the solvers to model airloads over an airfoil with a prescribed/simulated ice shape, collection efficiency modeling, ice growth, ice shedding, de-icing modeling, and assessment of the degradation of airfoil performance associated with the ice formation. Sample results have been shown to display the state of the art within these groups. While these results are encouraging, much additional work remains in modeling detailed physics important to rotorcraft icing phenomena. Despite these difficulties, progress in assessing helicopter ice accretion has been made and tools for initial analyses have been developed.
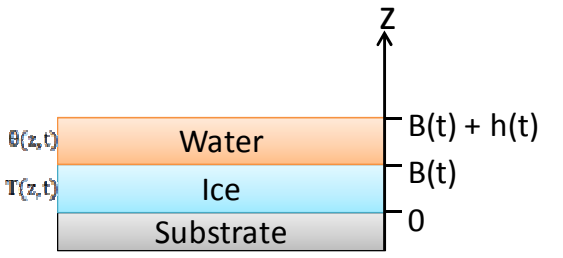
$$\frac{dT}{dt} = \frac{k_I}{\rho_I c_I} \frac{\partial^2 T}{\partial z^2}$$

Heat equation in the ice

$$\frac{d\theta}{dt} = \frac{k_w}{\rho_w c_w} \frac{\partial^2 \theta}{\partial z^2}$$

Heat equation in the water

$$\rho_i \frac{dB}{dt} + \rho_w \frac{dh}{dt} = \rho_a \beta V_\infty + \dot{m}_{in} - \dot{m}_{e,s}$$

Mass balance

$$\rho_I L_F \frac{dB}{dt} = k_I \frac{\partial T}{\partial z} - k_w \frac{\partial \theta}{\partial z}$$

Stefan condition at the ice / water interface

Schematic of the ice and water system

T, θ : Temperature t : time k_i, k_w : thermal conductivity of ice and water

$\rho_I, \rho_{w,} \rho_a$: density of ice, water and air c_I, c_w : specific heat of ice and water

B, h : thickness of ice and water layers $\rho_a \beta V_\infty$: impinging mass flow rate for a control volume

L_F : latent heat of solidification of water $\dot{m}_{in}$: runback mass flow rate for a control volume

$\dot{m}_{e,s}$: evaporating (or sublimating) mass flow rate for a control volume

Figure 3. Details of the Extended Messinger Model in One Dimension.
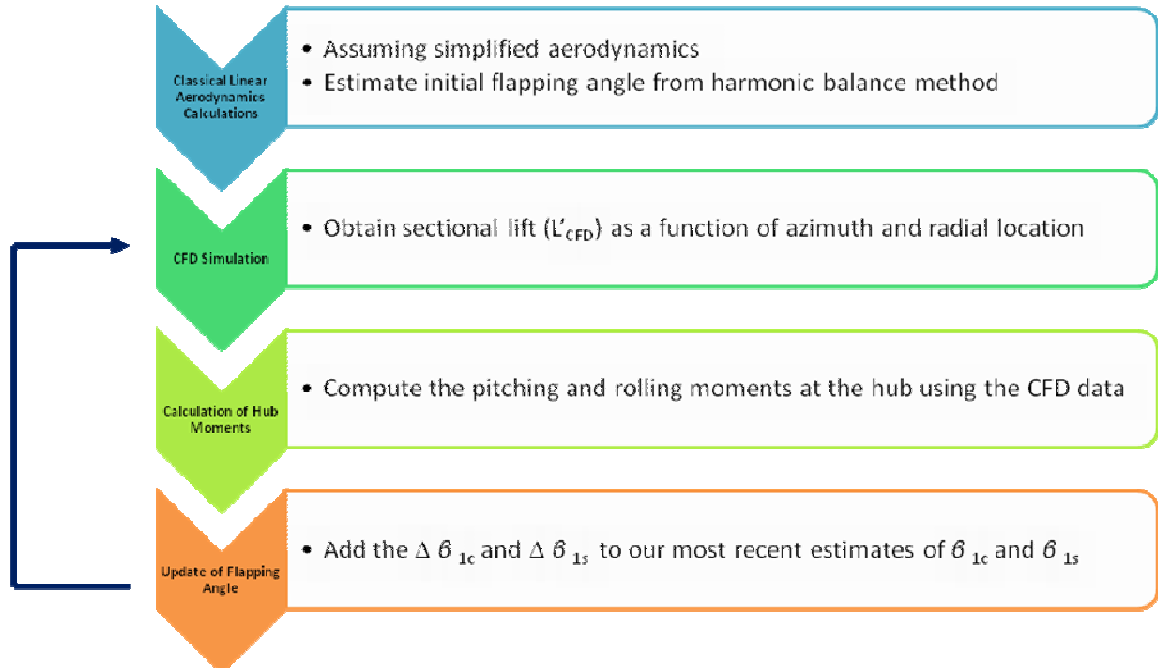
Figure 4. Flowchart of the CFD / Flapping Dynamics analysis.

6

Bell Tail Rotor
V_∞ = 60 knots, NR = 2100 RPM, T_∞ = 14°F, Collective = 8°, Shaft Tilt = -5°
LWC = 0.5 g/m³, Drop = 15 μm, Duration = 60 seconds
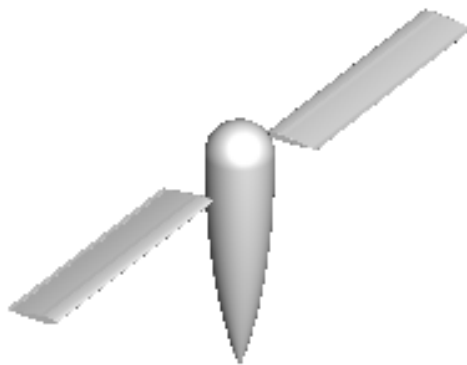
Black (Solid) : Clean
Green (Solid) : Experiment
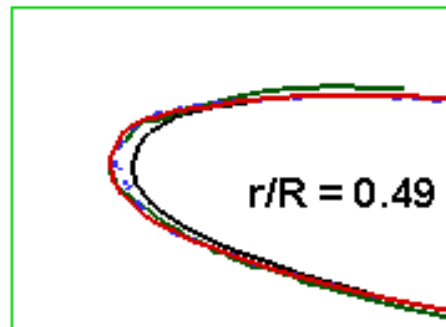Blue (Dashed) : LEWICE
Red (Solid) : Extended Messinger

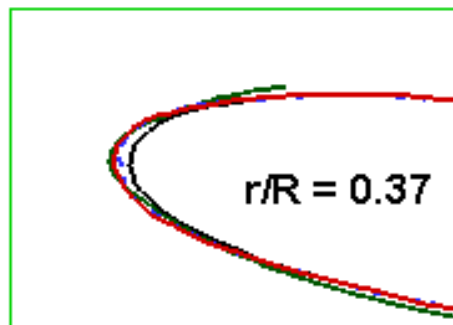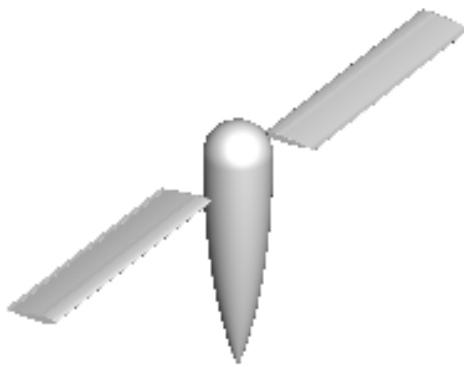r/R = 0.37
r/R = 0.49
r/R = 0.61
r/R = 0.74
r/R = 0.86
r/R = 0.98
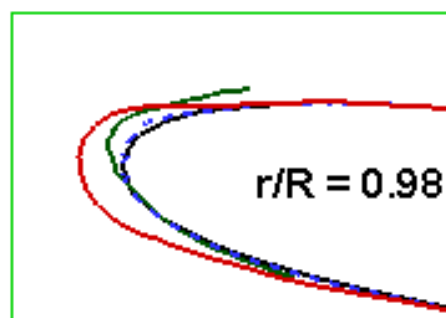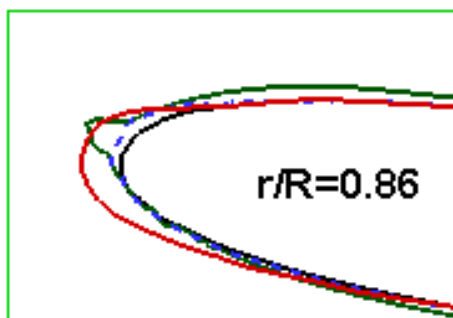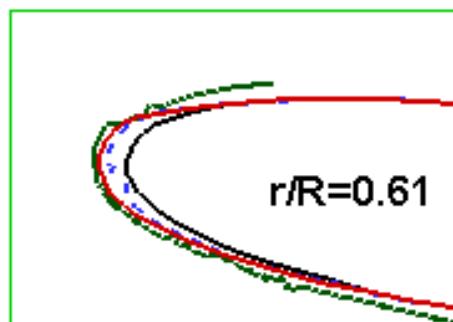
Figure 5. Comparisons of ice shape for Run54 (NASA Glenn's IRT).

Bell Tail Rotor
V_∞ = 60 knots, NR = 2100 RPM, T_∞ = 14° F, Collective = 8°, Shaft Tilt = -5°
LWC = 0.5 g/m³, Drop = 15 μm, Duration = 60 seconds

Black (Solid) : Clean
Green (Solid) : Experiment
Blue (Dashed) : w/o kinetic heating
Red (Solid) : with kinetic heating

r/R = 0.37

r/R = 0.49

r/R=0.61

r/R = 0.74

r/R=0.86

r/R = 0.98
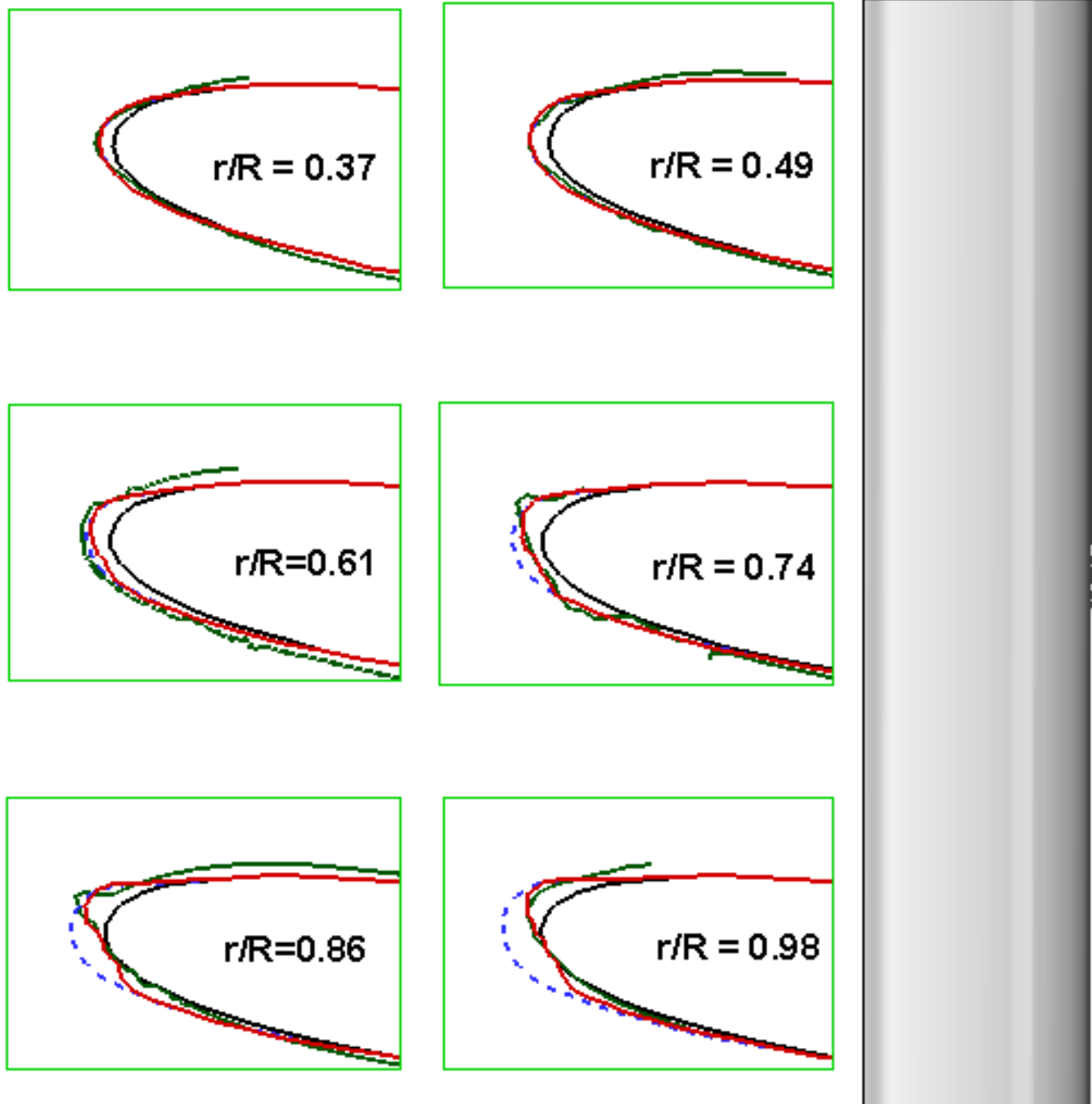
Figure 6. Comparisons of ice shape for Run54 (Kinetic heating effect, NASA Glenn's IRT).

8
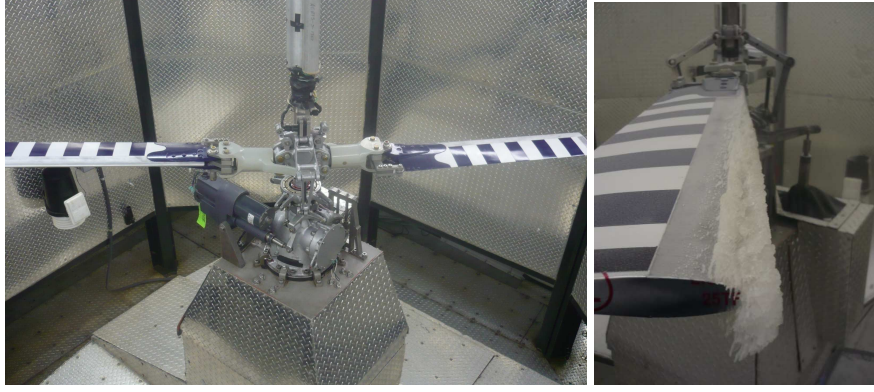
Figure 7. Photograph of AERTS facility and example of ice accretion shape.

□ Experiment
— Clean
— Extended Messinger
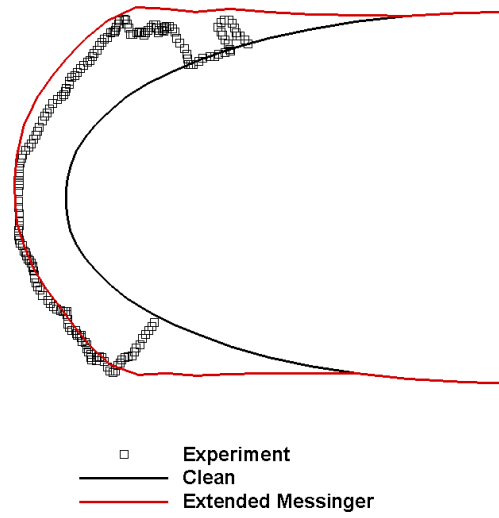
Figure 8. Comparisons of ice shape for Test4 (AERTS at Penn State).

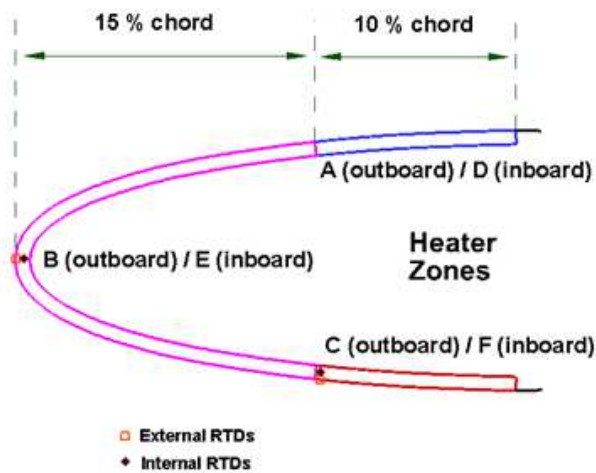(a) Shedding length

(b) Shedding time

(c) Ice thickness at tip
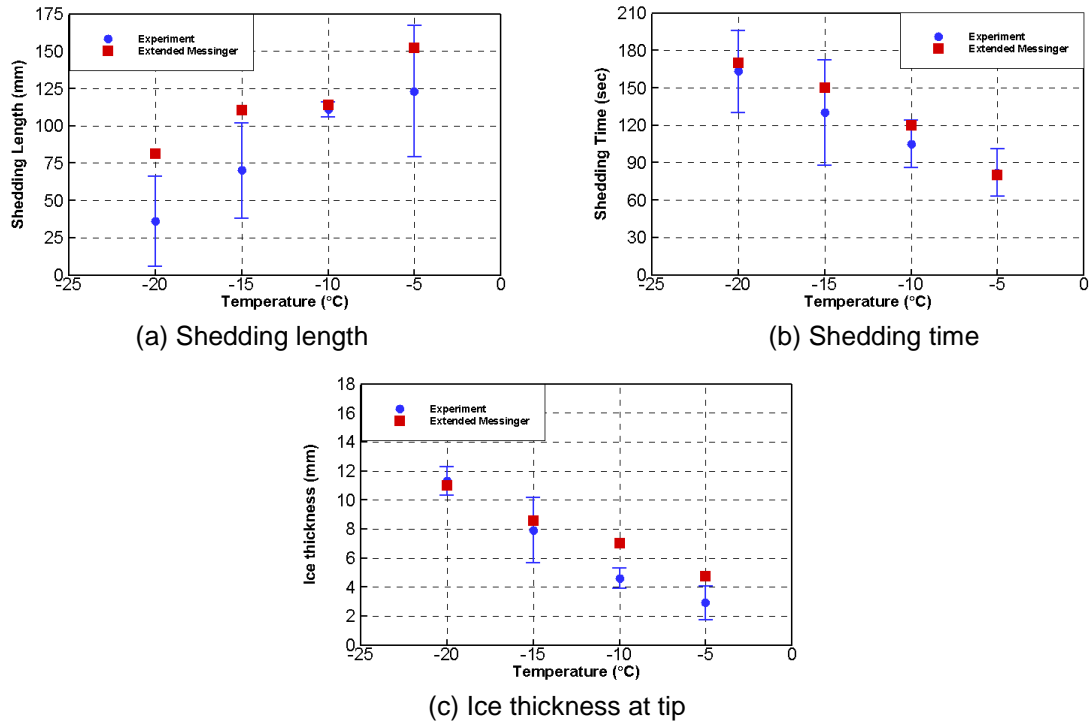
Figure 9. Comparison of predicted ice shedding properties with measurements (Fortin [25]).
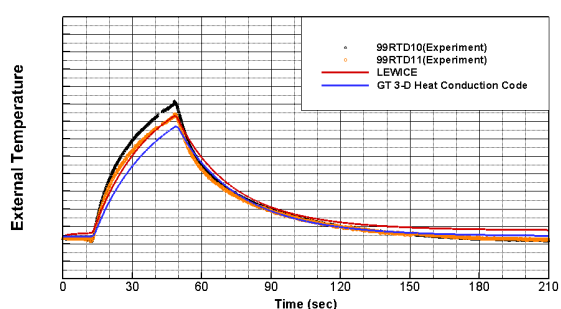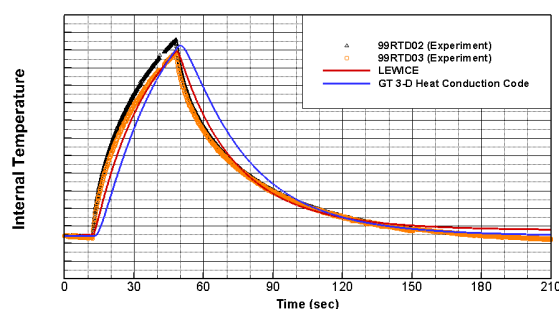
9

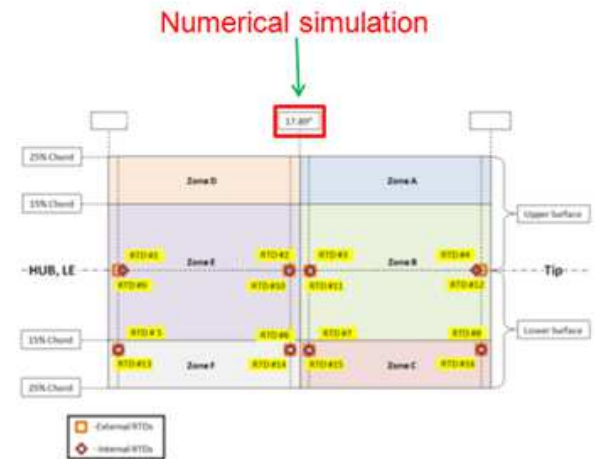Figure 10. Heater zone layout (NASA Glenn's IRT).

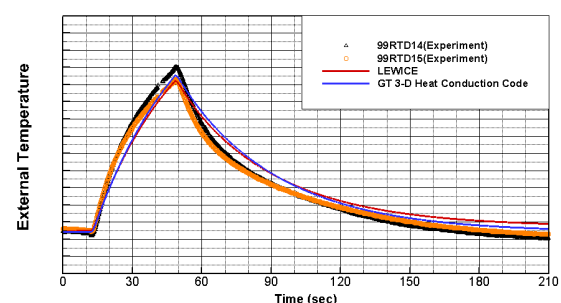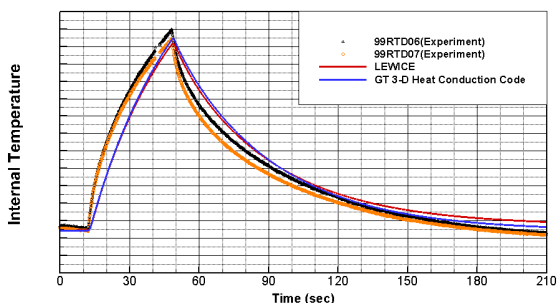Figure 11. Comparison of blade surface temperature at location B (NASA Glenn's IRT).

Figure 12. Comparison of blade surface temperature at location C (NASA Glenn's IRT).

REFERENCES

[1] Nucci, M., Bain, J., Sankar, L. N., Kreeger, R. E., Egolf, T. A., and Flemming, R.J., "Assessment of the Effects of Computational Parameters on Physics-based Models of Ice Accretion," 48th AIAA Aerospace Sciences Meeting, Orlando, FL, January 2010.

[2] Kim, J. W., Garza, D. P., Sankar, L. N., and Kreeger, R. E., "Ice Accretion Modelling using an Eulerian Approach for Droplet Impingement," 51st AIAA Aerospace Sciences Meeting, Grapevine, Texas, January 2013.

[3] Bain, J., Deresz, R., Sankar, L.N., Egolf, T. A., Flemming, R. J., and Kreeger, R. E., "Effects of Icing on Rotary Wing Loads and Surface Heat Transfer Rates," AIAA-2011-1100, 49th AIAA Aerospace Sciences Meeting including the New Horizons Forum and Aerospace Exposition, Orlando, Florida, Jan. 4-7, 2011.

[4] Kinzel, M. P., Noack, R. W., Sarofeen, C. M., Boger, D. A., Kreeger, R. E., "A CFD Approach for Predicting 3D Ice Accretion on Aircraft," SAE 2011-38-0044. Chicago, IL, June 13-17, SAE/AIAA/AHS International Conference on Aircraft and Engine Icing and Ground Deicing, 2011.

[5] Kinzel, M. P., Sarofeen, C. M., Noack, R. W., and Kreeger, R. E., "A Finite-Volume Approach to Modeling Ice Accretion," 28th AIAA Applied Aerodynamics Conference, Number AIAA-2010-4230, 2010.

[6] Sarofeen, C. M., Kinzel, M. P., Noack, R. W., and Kreeger, R. E., "A Numerical Investigation of Droplet/Particle Impingement on Dynamic Airfoils

and Rotor Blades," 28th AIAA Applied Aerodynamics Conference, 2010.

[7] Sarofeen, C. M., *Implementation and Validation of a Non-Cut-Cell Immersed Boundary Method for use in Icing Simulations*, M.S. Thesis, The Pennsylvania State University, University Park, PA, May 2011.

[8] Brown, C. M., Kunz, R.F., Lindau, J.W., Kinzel, M.P., "Assessment of turbulence modeling strategies for iced rotor configurations," Paper presented at 2nd Asian/Australian Rotorcraft Forum, Tianjin, China, September, 2013.

[9] Brown, C.M., *Computational Modeling of Rotor Blade Performance Degradation Due to Ice Accretions*, M.S. Thesis, The Pennsylvania State University, University Park, PA, December 2013.

[10] Wright, W. B., and Rutkowski, A., "Validation Results for LEWICE 2.0" [CD-ROM], NASA CR 1999208690, Jan. 1999.

[11] Wright, W. B., "Validation Results for LEWICE 3.0," NASA/CR-2005-213561; E-15007; AIAA Paper 2005-1243.

[12] Brouwers, E., Palacios, J., Smith, E., and Peterson, A., "The Experimental Investigation of a Rotor Hover Icing Model with Shedding," Presented at the American Helicopter Society 66th Annual Forum, Phoenix, AZ, May 11-13, 2010.

[13] Han, Y., Palacios, J., "Analytical and Experimental Determination of Airfoil Performance Degradation Due to Ice Accretion," AIAA 2012-2794.

[14] Rajmohan N., Sankar, L. N., Bauchau O., Charles B., Makinen S. M. and Egolf T. A., "Application of hybrid methodology to rotors in steady and maneuvering flight," in AHS 64th Annual Forum, 2008

[15] Wright, W. B., "User Manual for LEWICE Ver. 3.2," NASA CR 214255, Cleveland, OH, 2008.

[16] Hess J. L. and Smith A. M. O., "Calculation of potential flow about arbitrary bodies," *Progress in Aeronautical Sciences,* vol. 8, pp. 1-138, 1967.

[17] Frost W., "Two-dimensional particle trajectory computer program," Interim Report for Contract NAS3-22448, 1982.

[18] Messinger, B. L., "Equilibrium Temperature of an Unheated Icing Surface as a Function of Air Speed," Journal of the Aeronautical Sciences, Jan.1953, pp.29–42.

[19] Myers T. G., "Extension to the Messinger model for aircraft icing," AIAA Journal, Vol. 39, No. 2, 2001, pp. 211–218.

[20] Myers T. G., Charpin JPF, Thompson CP (2002), "Slowly accreting ice due to supercooled water impacting on a cold surface," Phys Fluids 14(1):240–256.

[21] Hill, J. M., *One-Dimensional Stefan Problems: An Introduction*, Longman Science Technical, Harlow, England, U.K., 1987, Chap. 1.

[22] Kreeger, R. E. And Tsao, J., "Ice Shapes on a Tail rotor," AIAA Paper 2014-2612, 6th AIAA Atmospheric and Space Environments Conference, Atlanta, GA, June 2014.

[23] Kreeger, R. E., Sankar, L. N., Nucci, M., and Kunz, R., "Progress in Rotorcraft Icing Computational Tool Development," SAE Technical Paper 2015-01-2088, 2015, doi:10.4271/2015-01-2088.

[24] Wright, J., Aubert, R., "Icing Wind Tunnel Test of a Full Scale Heated Tail Rotor Model," American Helicopter Society 71st Annual Forum, Virginia Beach, Virginia, May 5–7, 2015.

[25] Fortin, G. and Perron, J. "Spinning Rotor Blade Tests in Icing Wind Tunnel" Paper AIAA 2009-4260, 1st AIAA, Atmospheric and Space Environments Conference, San Antonio, TX, 2009.

Copyright Statement